Chemistry & Biology
Brief Communication

Tracing the Silhouette of Individual Cells in S/G_2/M Phases with Fluorescence

Asako Sakaue-Sawano,[1,2] Kenji Ohtawa,[3] Hiroshi Hama,[2] Masako Kawano,[4] Masaharu Ogawa,[4] and Atsushi Miyawaki[1,2,*]
[1]Life Function and Dynamics, ERATO, JST, 2-1 Hirosawa, Wako-city, Saitama 351-0198, Japan
[2]Laboratory for Cell Function and Dynamics, Advanced Technology Development Group, Brain Science Institute, RIKEN, 2-1 Hirosawa, Wako-city, Saitama 351-0198, Japan
[3]Brain Science Research Division, Brain Science and Life Technology, Research Foundation, 1-28-12 Narimasu, Itabashi, Tokyo 175-0094, Japan
[4]Laboratory for Cell Cuture Development, Brain Science Institute, RIKEN, 2-1 Hirosawa, Wako-city, Saitama 351-0198, Japan
*Correspondence: matsushi@brain.riken.go.jp
DOI 10.1016/j.chembiol.2008.10.015

SUMMARY

The APC^{Cdh1} E3 ligase is active in the late M and G_1 phases. Geminin is a direct substrate of the APC^{Cdh1} complex, and accumulates during the S, G_2, and M phases. By fusing the amino-terminal region of Geminin to fluorescent proteins, we have developed cell cycle markers that accumulate in the S/G_2/M phases in both the nucleus and the cytoplasm. These markers reveal the morphology of individual cells that have undergone DNA replication, allowing us to monitor cell growth relative to differentiation of various cell types. After electroporating the developing mouse embryos, we highlighted neuroepithelial progenitors in the S/G_2/M phases, which possessed an elongated morphology with an apical and/or a basal attachment. We also show that nuclear localization of the ubiquitin ligase for Geminin is essential for full performance of the markers.

INTRODUCTION

Fucci is a fluorescent cell cycle indicator that harnesses the ubiquitination oscillators that control cell-cycle transitions (Sakaue-Sawano et al., 2008). The original Fucci probe was generated by fusing mAG (monomeric Azami Green) and mKO2 (monomeric Kusabira Orange2) to ubiquitination domains of human Geminin (McGarry and Kirschner, 1998) and Cdt1 (Nishitani et al., 2000), respectively. These two chimeric proteins, mAG-hGem(1/110) and mKO2-hCdt1(30/120), accumulate reciprocally in the nucleus of transfected cells during the cell cycle, labeling the nuclei of S/G_2/M phase cells green and those in G_1 phase red (see Figure S1 available online). We generated cultured cells and transgenic mice constitutively expressing Fucci, in which every cell nucleus exhibits either red or green fluorescence (Sakaue-Sawano et al., 2008). We performed time-lapse imaging to explore the spatiotemporal patterns of cell-cycle dynamics during the epithelial-mesenchymal transition of cultured cells, the migration and differentiation of neural progenitors in brain slices, and the development of tumors across blood vessels in live mice. However, nuclear targeting of fluorescence signal has both benefits and drawbacks. While it is easy to identify individual nuclei, it is difficult to identify cell types and differentiation states by their characteristic morphologies. In this study, we tried to locate Fucci signals, in the cytoplasm in order to trace the silhouette of individual cells with fluorescence in a cell cycle-dependent manner.

RESULTS AND DISCUSSION

In order to visualize overall cell morphology using Fucci, we examined other truncated versions of Geminin and Cdt1 proteins for cytoplasmic expression. Each construct was stably expressed in HeLa cells using a lentiviral expression system, and examined for cell-cycle dependency and distribution pattern. Truncation of the 50 carboxyl-terminal amino acids of mAG-hGem(1/110) resulted in delocalization of the green fluorescence, as shown in our previous report (Sakaue-Sawano et al., 2008); thus, mAG-hGem(1/60) is an S/G_2/M marker distributed in both the nucleus and the cytoplasm. As was the case for hGem(1/110), hGem(1/60) could be fused to other fluorescent proteins (Sakaue-Sawano et al., 2008). For instance, a yellow monomeric variant of *Aequorea* GFP (mVenus) (Nagai et al., 2002) and a red monomeric fluorescent protein (mCherry) (Shaner et al., 2004) could be substituted for mAG to generate mVenus-hGem(1/110), mVenus-hGem(1/60), mCherry-hGem(1/110), and mCherry-hGem(1/60). While mVenus-hGem(1/110) and mCherry-hGem(1/110) accumulated only in the nucleus, mVenus-hGem(1/60) and mCherry-hGem(1/60) were detected in both the nucleus and the cytoplasm (Figure 1, DIC + FL). More importantly, the S/G_2/M specificity of these constructs was confirmed by measuring the DNA content of transformed cells using fluorescence-activated cell sorting (FACS) (Figure 1, Hoechst33342 and cell-cycle profile). We also obtained HeLa cells that constitutively express equivalent levels of mKO2-hCdt1(30/120) and mAG-hGem(1/60) to observe that green fluorescence alternated with red fluorescence (Figure S2). By contrast, we have not been able to truncate Cdt1 so that the G_1 specific signal is distributed in the cytoplasm as well as the nucleus. We therefore focused on Geminin-based markers in this study, which by themselves can provide in vivo information about cell proliferation patterns (Sakaue-Sawano et al., 2008). For clarity, we have adopted a nomenclature that provides

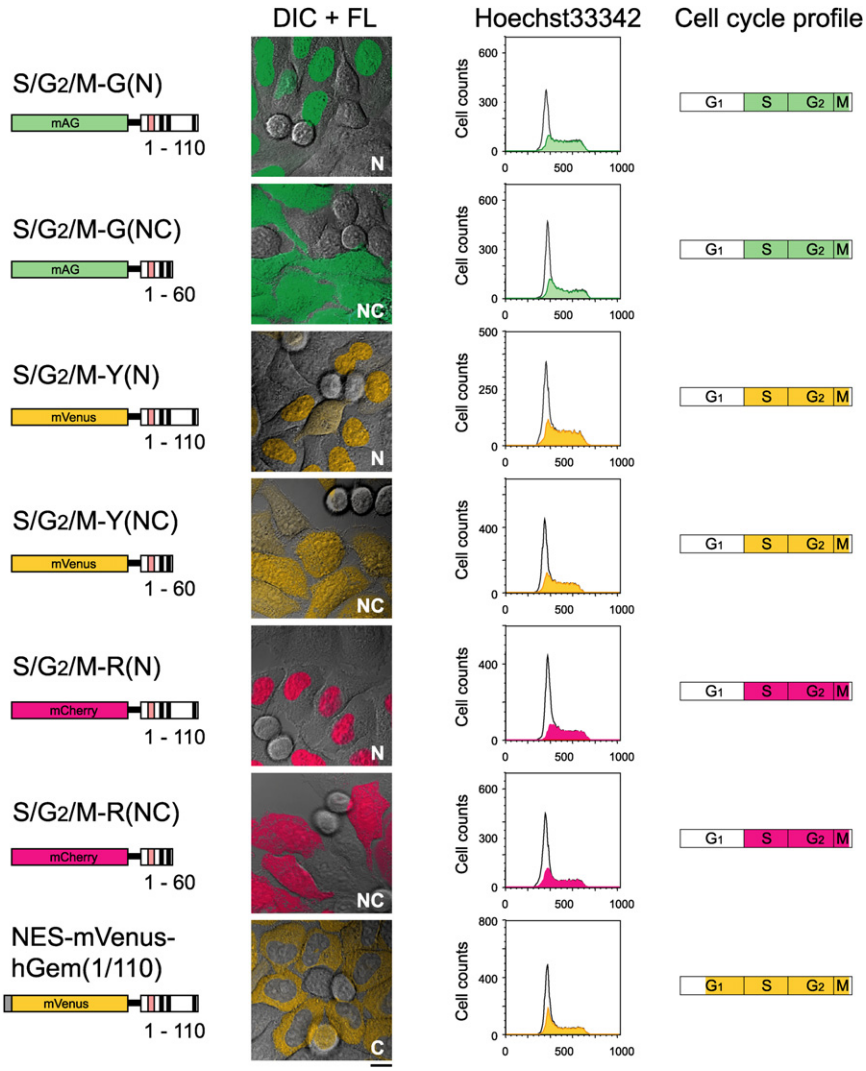

Figure 1. S/G_2/M Markers with Different Colors and Distribution Patterns

Various constructs with concatenated fluorescent proteins (mAG, mVenus, or mCherry) fused to deletion mutants of human Geminin for labeling cells in S, G_2, and M phases. Pink box, D (destruction) box; black box, NLS (nuclear localization signal).

(DIC + FL) Typical differential interference contrast (DIC) and fluorescence (FL) images of HeLa cells stably expressing constructs. Distribution patterns are indicated as follows: N, nucleus; C, cytosol; NC, nucleus and cytosol. Scale bar, 10 μm.

(Hoechst33342) HeLa cells stably expressing S/G_2/M markers were stained with Hoechst33342 and analyzed using fluorescence-activated cell sorting.

(Cell cycle profile) Cell cycle phases highlighted by fluorescence are colored.

information about the marker properties, including color (G, green; Y, yellow; R, red) and distribution (N, nuclear; C, cytoplasmic; NC, nuclear and cytoplasmic). As shown in Figure 1, mAG-hGem(1/110), mAG-hGem(1/60), mVenus-hGem(1/110), mVenus-hGem(1/60), mCherry-hGem(1/110), and mCherry-hGem(1/60) were renamed S/G_2/M-G(N), S/G_2/M-G(NC), S/G_2/M-Y(N), S/G_2/M-Y(NC), S/G_2/M-R(N), and S/G_2/M-R(NC), respectively.

To examine whether these markers can outline the silhouette of differentiating and migrating cells, we first focused on neural progenitor cells in the developing cerebral cortex. While progressing through the cell cycle, these cells gain and lose processes and displace their nuclei within the cytoplasm. Plasmid DNA for S/G_2/M-R(NC) was transferred to the cerebral cortex of embryonic mouse brains (E13) using an electroporation technique (Tabata and Nakajima, 2001). One day post-DNA transfer, fixed sections were prepared and immunostained for Tuj1, a neuronal marker (Ferreira and Caceres, 1992). S/G_2/M-R(NC) fluorescence was observed in some mitotic neural progenitors in the ventricular zone, but not in cortical plate postmitotic neurons that were heavily immunostained for Tuj1 (Figure 2A). The fluorescent neural progenitors were supposed to be in S/G_2/M phases and could be classified into two groups. First, surface-dividing progenitor cells generate paired cycling daughter cells through division on the ventricular surface (Figure 2B). Their nuclear movement is known as interkinetic nuclear migration (Sauer, 1935); M-phase nuclei are located on the ventricular surface, while S-phase nuclei are located far from the ventricle. These progenitor cells extend both basal and apical processes, while their nuclei descend in the ventricular zone (Figure 2B). Second, non-surface-dividing progenitor cells undergo mitosis that generates neurons near the intermediate zone, possibly to efficiently supply the cortical plate with neurons (Noctor et al., 2004). These cells lose apical or basal processes before entering M phase (Figure 2C) (Miyata et al., 2004). Because most neural progenitor cells possess an elongated morphology with a basal attachment, it will be interesting to perform time-lapse observations of the developing cortical surface to visualize cell-cycle progression that occurs in deep regions.

Next, we used neurospheres, which are free-floating aggregates that provide an in vitro model system, to investigate the mechanisms underlying the maintenance, proliferation, and differentiation of neural progenitor cells (Shetty and Turner, 1998). Migration of mitotic neural progenitor cells is observed when neurospheres are plated (chain migration) (Jacques et al., 1998). A lentivirus encoding S/G_2/M-R(N) or S/G_2/M-R(NC) was transduced into rat neurospheres, which were then plated onto poly-L-lysine-coated glass-bottom dishes (Figure 2D and Figure S3). Cells expressing S/G_2/M-R(N) had red nuclei, while red fluorescence was observed throughout S/G_2/M-R(NC)-transduced cells in a cell-cycle-dependent manner. This labeling allows us to identify cells in S/G_2/M phases by observing cellular processes and to monitor how neural progenitor cells differentiate during chain migration from neurospheres.

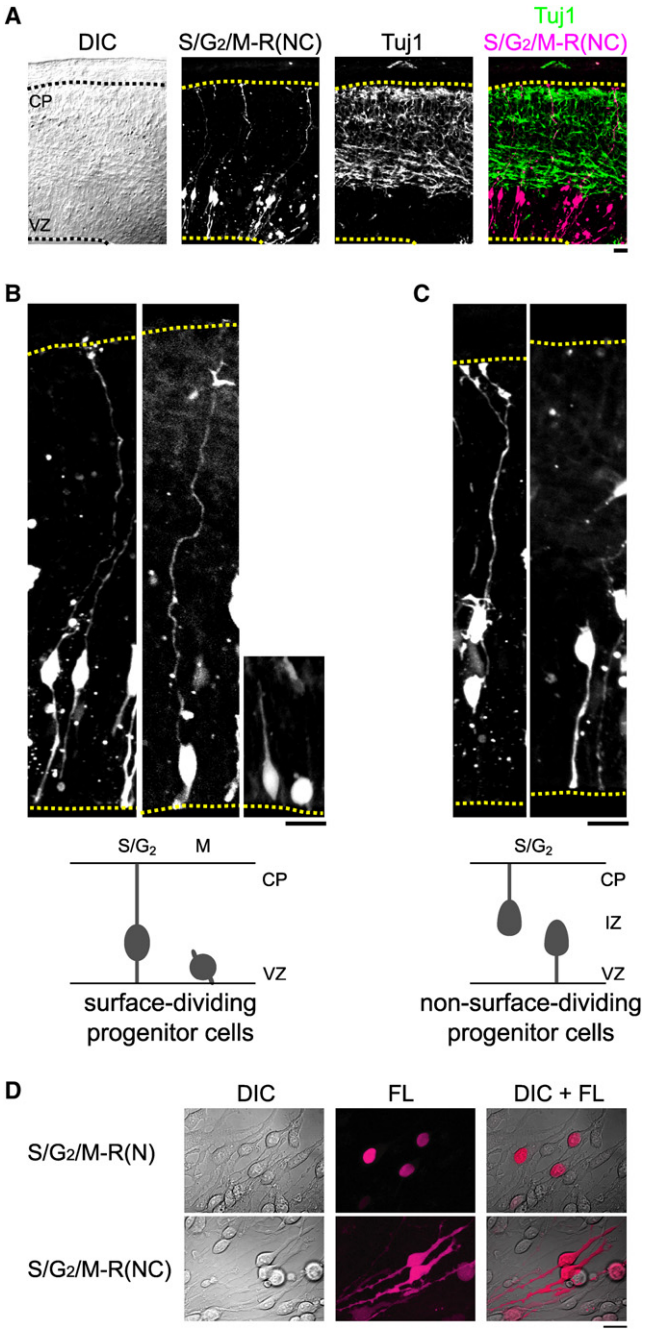

Figure 2. S/G_2/M Markers in Neural Progenitor Cells

(A–C) Immunohistochemical observation of neural progenitor cells expressing S/G_2/M-R(NC) in developing cerebral cortex. In utero electroporation was performed on mouse embryos at E13, and, one day later, red fluorescence of S/G_2/M-R(NC) was observed in sections prepared from dorsal telencephalon. (A) DIC and FL images of a section incubated with anti-Tuj1 mAb. Red and green signals for S/G_2/M-R(NC) and Tuj1, respectively, are superimposed (right). Scale bar, 20 μm. CP, cortical plate; VZ, ventricular zone.

(B and C) High magnification images of fluorescent neural progenitor cells before surface-division (B) and non-surface-division (C). Scale bar, 20 μm. CP, cortical plate; IZ, intermediate zone; VZ, ventricular zone. The morphology of mitotic neural progenitor cells in S/G_2/M phases is schematized (bottom).

(D) DIC and FL images of S/G_2/M-R(N) (top) and S/G_2/M-R(NC) (bottom), expressing cells migrating from neurospheres. Scale bar, 20 μm.

Since the ubiquitination and degradation of Geminin depends on its subcellular localization, it is likely that the performance of Fucci probes is also affected by subcellular localization. In order to study the molecular dynamics of the S/G_2/M markers containing mVenus, we performed photobleaching experiments (Lippincott-Schwartz et al., 2003) using laser-scanning confocal microscopy. First, we carried out a FLIP (fluorescence loss during photobleaching) experiment to examine the mobility of S/G_2/M-Y(N) inside the nucleus. While a region was photobleached, substantial loss of fluorescence was observed in the rest of the nucleus (Figure 3A), indicating that the marker is mobile. It is thus likely that S/G_2/M-Y(N) is not bound to chromatin, consistent with the fact that the marker spreads throughout the entire cell as soon as the nuclear envelope is broken down in M phase (Figure S4). The N-terminal region (residues 1–110) of Geminin has several clusters of Arg and Lys residues, which presumably function as a nuclear localization signal (NLS). Because S/G_2/M-Y(NC) is uniformly distributed in both cytosolic and nuclear compartments, it is probable that an RRK sequence at residues 106–108 is essential for nuclear localization (Boos et al., 2006) of S/G_2/M-Y(N).

Next, we carried out a FRAP (fluorescence recovery after photobleaching) experiment on cells expressing S/G_2/M-Y(NC) to examine movement of the probe between the nucleus and the cytoplasm (Figure 3B). A substantial gradient of fluorescence signal was apparent across the nuclear envelope immediately after the whole nuclear region was photobleached. The relative distribution between the two compartments reached equilibrium within 6–8 min after photobleaching. This indicates that S/G_2/M-Y(NC) shuttles effectively across the nuclear envelope.

Finally, since access to E3 ligase and proteasome activity is crucial for regulation of Geminin function and therefore is likely to affect the function of Fucci probes, we examined the immunocytochemical localization of the enzyme complexes responsible for ubiquitination and degradation of Geminin using antibodies against a component of APC/C (APC2) (Gieffers et al., 1999) and the 20S proteasome (Rockel et al., 2005), respectively. While signal for 20S proteasome was detected in both the nucleus and cytoplasm, APC2 signal was confined to the nucleus (Figure S5). The differential distribution of the two signals was apparent in all phases of the cell cycle (Figure 4). In addition, S/G_2/M markers showed decreased cell-cycle specificity when excluded from the nucleus by the addition of a nuclear export signal (NES); the fluorescence of NES-mVenus-hGem(1/110) emerged in the middle of the G_1 phase (Figure 1A). Thus, it is likely that the Geminin-based probes require APC/C inside the nucleus for optimal performance. S/G_2/M markers made from hGem(1/60) may also be degraded, due to their efficient nucleocytoplasmic shuttling.

SIGNIFICANCE

The S/G_2/M marker of the original Fucci probe consists of mAG and an ubiquitination domain of human Geminin. The chimeric protein mAG-hGem(1/110) accumulates in the nuclei of transfected cells during the cell cycle, labeling nuclei of S/G_2/M phase cells green. The development of Fucci derivatives has benefited from the exploration of the molecular mechanisms underlying ubiquitin-mediated protein degradation. Since access to E3 ubiquitin ligase

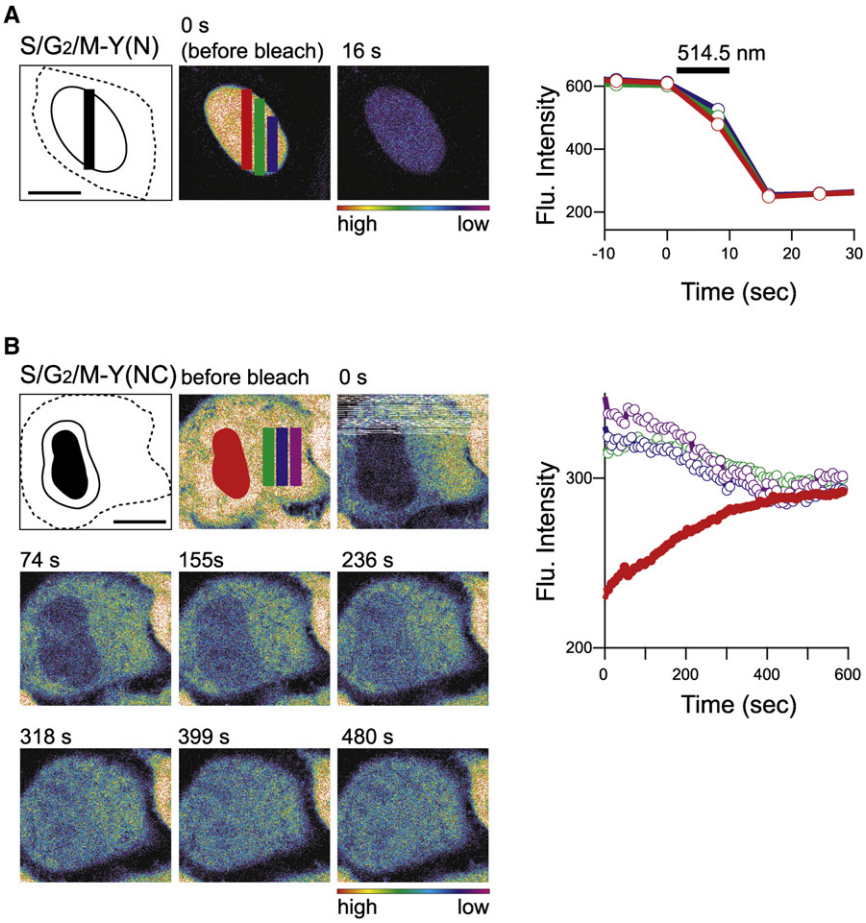

Figure 3. Mobility of S/G_2/M Markers

(A) High mobility of S/G_2/M-Y(N) within the nucleus of HeLa cells revealed by a FLIP (fluorescence loss during photobleaching) experiment. Left: During t = 0–16 s, a rectangular region (filled in black in the scheme) was irradiated by a full power laser line (514.5 nm). Confocal images were acquired with excitation at 488 nm every 8 s. Fluorescence intensity images (pseudocolor) at 0s and 16 s are shown. The average intensities in three rectangular regions (red, green, and blue) were measured. The red rectangle corresponds to the photobleached region. Scale bar, 10 μm. Right: Temporal profiles of the average fluorescence intensities in the red, green, and blue rectangular regions (the 0s image) are shown in red, green, and blue, respectively.

(B) Efficient shuttling of S/G_2/M-Y(NC) between the nucleus and the cytoplasm revealed by a FRAP (fluorescence recovery after photobleaching) experiment. Left: The fluorescent marker inside the nucleus was photobleached by applying strong 514.5 nm irradiation to the region shown in black. Confocal images were acquired with excitation at 488 nm every 8s. Fluorescence intensity images (pseudocolored) at 0s, 74s, 155s, 236s, 318s, 399s, and 480s are shown. The average intensities in the photobleached region (red) and three rectangular regions (green, blue, and violet) were measured. Scale bar, 10 μm. Right: Temporal profiles of the average fluorescence intensities in the four regions are drawn in red, green, blue, and violet, respectively.

and proteasome activity is crucial for the performance of the cell-cycle probe, we examined the immunocytochemical localization of enzyme complexes responsible for the ubiquitination and degradation of Geminin. While the degradation machinery was distributed in both the cytoplasm and the nucleus, the ubiquitination system was concentrated in the nucleus. Thus, the S/G_2/M marker functions best in the nucleus.

In the present study, however, the marker was successfully delocalized throughout the cell by further truncation of the Geminin domain. Because the new marker, mAG-hGem(1/60), was not bound to chromatin and because it shuttled between cytoplasm and nucleus quickly, its existence inside the nucleus ensured cell-cycle-dependent proteolysis. Thus, mAG-hGem(1/60) can reveal the morphology of individual cells that have undergone DNA replication, allowing us to monitor cell growth relative to the differentiation of various cell types. We have also expanded the S/G_2/M marker family by replacing mAG with mVenus or mCherry in order to increase color variation. Using these probes, we outlined the silhouette of neural progenitor cells in S/G_2/M phases in the developing cerebral cortex. Our study provides an important guide for the development and improvement of indicators based on ubiquitin-mediated proteolysis.

EXPERIMENTAL PROCEDURES

Gene Construction

cDNAs encoding mVenus (Nagai et al., 2002), and mCherry (Shaner et al., 2004) were amplified using primers containing 5′-*Eco*RI and 3′-*Eco*RV sites, and digested products were substituted for mAG gene of pcDNA3/mAG-hGeminin(1/110) vector (Sakaue-Sawano et al., 2008) to generate pcDNA3/mVenus-hGeminin(1/110) and pcDNA3/mCherry-hGeminin(1/110), respectively. cDNA-encoding S/G_2/M markers (hGeminin(1/110)) were cloned into the *Eco*RI/*Xba*I sites of the CSII-EF-MCS vector to generate CSII-EF-MCS/mVenus-hGeminin(1/110) and CSII-EF-MCS/mCherry-hGeminin(1/110). The partial cDNA fragments of human Geminin (1/60) (GenBank: NM_015895) were amplified using primers containing 5′-*Not*I and 3′-*Xba*I sites, and digested products were substituted for hGeminin(1/110) gene at the *Not*I/*Xba*I sites of CSII-EF-MCS/mAG-hGeminin(1/110), CSII-EF-MCS/mVenus-hGeminin(1/110), or CSII-EF-MCS/mCherry-hGeminin(1/110) to generate CSII-EF-MCS/mAG-hGeminin(1/60), CSII-EF-MCS/mVenus-hGeminin(1/60), or CSII-EF-MCS/mCherry-hGeminin(1/60).

Cell Culture

HeLa.S cells were grown in DMEM that was supplemented with 10% fetal bovine serum and penicillin/streptomycin.

Lentivirus Production

Replication-defective, self-inactivating lentiviral vectors were used (Miyoshi et al., 1998; Sakaue-Sawano et al., 2008). The CSII-EF-MCS vector encoding an S/G_2/M marker was cotransfected with the packaging plasmid (pCAG-HIVgp), the VSV-G-, and Rev-expressing plasmid (pCMV-VSV-G-RSV-Rev)

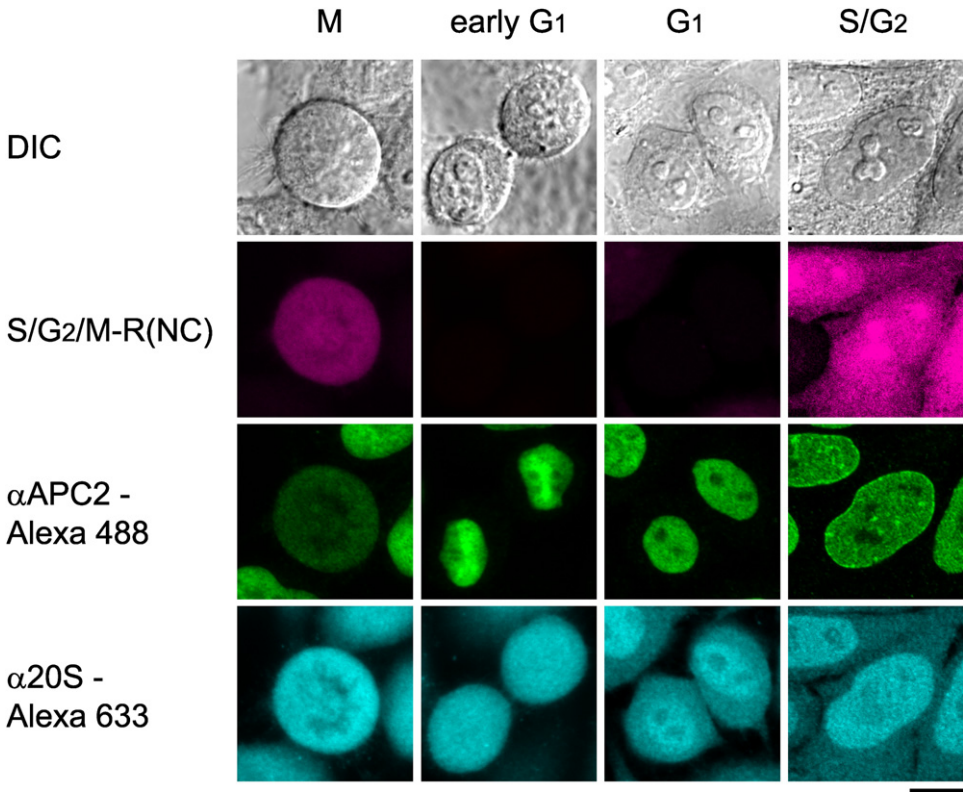

Figure 4. Localization of Ubiquitination and Degradation of Geminin
Immunocytochemical localization of APC2 and 20S proteasome in S/G2/M-R(NC)-expressing HeLa cells at different cell cycle phases. Anti-APC2 polyclonal antibody (SantaCruz, SC-20984) and anti-20S proteasome alpha-subunits monoclonal antibody (BIOMOL, PW8195) were used with Alexa 488- and Alexa 633-conjugated secondary antibodies, respectively. Scale bar, 10 μm.

into 293T cells. High-titer viral solutions for the markers were prepared and used for transduction into HeLa cells or neurospheres.

Imaging of Cultured Cells

Cells stably expressing an S/G_2/M marker were grown on a 35-mm glass-bottom dish in phenol red-free Dulbecco's modified Eagle's medium containing 10% fetal bovine serum (FBS). Cells were subjected to long-term, time-lapse imaging using a computer-assisted fluorescence microscope (Olympus, Tokyo, Japan; LCV100) equipped with an objective lens (Olympus, UAPO 40X/340 N.A. = 0.90), a halogen lamp, a red LED (620 nm), a CCD camera (Olympus, DP30), differential interference contrast (DIC) optical components, and interference filters. For fluorescence imaging, the halogen lamp was used with a 470DF35 excitation filter, a 505DRLP dichroic mirror, and a 510WB40 emission filter for observing mAG; a 490DF20 excitation filter, a 525DRLP dichroic mirror, and a 545AF35 emission filter for observing mVenus; and a 565WB20 excitation filter, a 595DRLP dichroic mirror, and a 635DF55 emission filter for observing mCherry. For DIC imaging, the red LED was used with a filter cube containing an analyzer. Image acquisition and analysis were performed using MetaMorph 6.37 software (Universal Imaging, Media, PA).

Immunocytochemistry

HeLa cells were fixed with 4% PFA for 10 min at 4°C and then permeabilized in 0.1% Triton X-100/phosphate-buffered saline for 10 min at room temperature. The antibodies used were: anti-APC2 polyclonal antibody (SantaCruz, SC-20984), anti-20S proteasome alpha-subunits monoclonal antibody (BIOMOL, PW8195), Alexa Fluor 488-conjugated goat anti-rabbit IgG (Molecular Probes), and Alexa Fluor 633-conjugated goat anti-mouse IgG (Molecular Probes). Image acquisition was performed using an FV1000 (Olympus) confocal microscope system equipped with 488 nm (argon), 559 nm (laser diode), and 635 nm (laser diode) laser lines.

Flow Cytometry

Hoechst 33342 solution (56 μl of 1 mg/ml stock) (DOJINDO) was added to a 10-cm dish containing Fucci-expressing HeLa cells. After incubation for 30 min, cells were harvested and analyzed using a FACSAria II (BD Bioscience, San Jose, CA). mAG and mVenus were excited by a 488-nm laser line (laser diode) and their emissions were collected through 515/20BP; mCherry was excited by a 532-nm laser line (diode-pumped solid state laser) and its emission was collected through 610/20 BP. Hoechst 33342 was excited by a UV Laser at 355 nm, and fluorescence signal was collected through 405/20 BP. The data were analyzed using FlowJo software (Tree Star, Ashland, OR).

Electroporation and Immunohistochemistry

The experimental procedures and housing conditions for animals were approved by the Institute's Animal Experimental Committee, and all animals were cared for and treated humanely in accordance with the Institutional Guidelines for Experiments Using Animals. At E13, pregnant mice were deeply anesthetized, and the uterine horns were exposed onto phosphate-buffered saline (PBS)-moistened cotton gauze. Approximately 1 μl of plasmid DNA solution (1-5 μg/μl) for S/G_2/M-R(NC) was injected into the ventricle via a pulled-glass capillary. Then, electrodes (CUY 650-5; Nepa Gene, Chiba, Japan) were placed on both sides of each embryo and electroporation was performed using a square electroporator CUY21 EDIT (Nepa Gene), as described previously (Tabata and Nakajima, 2001). The uterine horns were placed back into the abdominal cavity to allow the embryos to continue normal development. One day later, embryos were perfused transcardially with fixative (4% PFA), placed in ice-cold fixative for 2 hr, cryoprotected in PBS containing 20% sucrose, and embedded in

OCT compound. Coronal head sections (15 μm thick) were incubated with anti-Tuj1 mAb (Covance), followed by rabbit-anti-mouse IgG conjugated with AlexaFluor 488 (Molecular Probes). Sections were imaged using FV1000 (Olympus) confocal microscope system equipped with two laser diodes: 473 nm and 559 nm.

Neurospheres

Cell suspension prepared from the hippocampi of rat embryos (E16) was exposed to a Lentivirus-encoding S/G_2/M-R(N) or S/G_2/M-R(NC). Primary neurospheres were formed in the growth medium containing DMEM/F-12 (Invitrogen), 0.5% horse serum (Sigma), basic FGF (20 ng/ml) (R&D systems), and N2 supplement (Invitrogen). Neurospheres were plated onto poly-L-lysine-coated glass-bottom dishes. After 90 min, the growth medium was replaced with new one (except for horse serum) and then subjected to imaging experiments.

SUPPLEMENTAL DATA

Supplemental Data include five figures and can be found with this article online at http://www.cell.com/chemistry-biology/supplemental/S1074-5521(08)00420-1/.

ACKNOWLEDGMENTS

The authors thank Mayu Sugiyama and Hiroshi Kurokawa for technical assistance, and Hideaki Mizuno, Noriko Ohsumi, and Hiroyuki Miyoshi for valuable advice. mCherry was kindly provided by R.Y. Tsien. This work was partly supported by grants from Japan MEXT Grant-in-Aid for Scientific Research on priority areas and the Human Frontier Science Program (HFSP).

Received: July 21, 2008
Revised: October 15, 2008
Accepted: October 30, 2008
Published: December 19, 2008

REFERENCES

Boos, A., Lee, A., Thompson, D.M., Jr., and Kroll, K.L. (2006). Subcellular translocation signals regulate Geminin activity during embryonic development. Biol. Cell *98*, 363–375.

Ferreira, A., and Caceres, A. (1992). Expression of the class III β-tubulin isotype in developing neurons in culture. J. Neurosci. Res. *32*, 516–529.

Gieffers, C., Peters, B.H., Kramer, E.R., Dotti, C.G., and Peters, J.M. (1999). Expression of the CDH1-associated form of the anaphase-promoting complex in postmitotic neurons. Proc. Natl. Acad. Sci. USA *96*, 11317–11322.

Jacques, T.S., Relvas, J.B., Nishimura, S., Pytela, R., Edwards, G.M., Streuli, C.H., and French-Constant, C. (1998). Neural precursor cell chain migration and division are regulated through different beta1 integrins. Development *125*, 3167–3177.

Lippincott-Schwartz, J., Altan-Bonnet, N., and Patterson, G.H. (2003). Photobleaching and photoactivation: following protein dynamics in living cells. Nat. Cell Biol. (*Suppl*), S7–S14.

McGarry, T.J., and Kirschner, M.W. (1998). Geminin, an inhibitor of DNA replication, is degraded during mitosis. Cell *93*, 1043–1053.

Miyata, T., Kawaguchi, A., Saito, K., Kawano, M., Muto, T., and Ogawa, M. (2004). Asymmetric production of surface-dividing and nonsurface-dividing cortical progenitor cells. Development *131*, 3133–3145.

Miyoshi, H., Blömer, U., Takahashi, M., Gage, F.H., and Verma, I.M. (1998). Development of a self-inactivating lentivirus vector. J. Virol. *72*, 8150-5-8157.

Nagai, T., Ibata, K., Park, E.S., Kubota, M., Mikoshiba, K., and Miyawaki, A. (2002). A variant of yellow fluorescent protein with fast and efficient maturation for cell-biological applications. Nat. Biotechnol. *20*, 87–90.

Nishitani, H., Lygerou, Z., Nishimoto, T., and Nurse, P. (2000). The Cdt1 protein is required to license DNA for replication in fission yeast. Nature *404*, 625–628.

Noctor, S.C., Martinez-Xerdeno, V., Ivic, L., and Kriegstein, A.R. (2004). Cortical neurons arise in symmetric and asymmetric division zones and migrate through specific phases. Nat. Neurosci. *7*, 136–144.

Rockel, T.D., Stuhlmann, D., and von Mikecz, A. (2005). Proteasomes degrade proteins in focal subdomains of the human cell nucleus. J. Cell Sci. *118*, 5231–5242.

Sauer, F.C. (1935). Mitosis in the neural tube. J. Comp. Neurol. *62*, 377–405.

Sakaue-Sawano, A., Kurokawa, H., Morimura, T., Hanyu, A., Hama, H., Osawa, H., Kashiwagi, S., Fukami, K., Miyata, T., Miyoshi, H., et al. (2008). Visualizing spatiotemporal dynamics of multicellular cell-cycle progression. Cell *132*, 487–498.

Shaner, N.C., Campbell, R.E., Steinbach, P.A., Giepmans, B.N., Palmer, A.E., and Tsien, R.Y. (2004). Improved monomeric red, orange, and yellow fluorescent proteins derived from Discosoma sp. Red fluorescent protein. Nat. Biotechnol. *22*, 1567–1572.

Shetty, A.K., and Turner, D.A. (1998). In vitro survival and differentiation of neurons derived from epidermal growth factor-responsive postnatal hippocampal stem cells: inducing effects of brain-derived neurotrophic factor. J. Neurobiol. *35*, 395–425.

Tabata, H., and Nakajima, K. (2001). Efficient in utero gene transfer system to the developing mouse brain using electroporation: visualization of neuronal migration in the developing cortex. Neuroscience *103*, 865–872.

